Probing Isomers and Conformers by Cryogenic Ion Vibrational Spectroscopy: Deprotonated States of Valine and Aminovaleric Acid

*Lane M. Terry,[1] Maddie K. Klumb,[1] Deacon J. Nemchick,[2] Robert P. Hodyss,[2] and J. Mathias Weber[1,]**

[1] JILA and Department of Chemistry, University of Colorado Boulder, 440 UCB, Boulder, CO 80309-0440, USA

[2] Jet Propulsion Laboratory, California Institute of Technology, Pasadena, CA, USA

TOC Figure

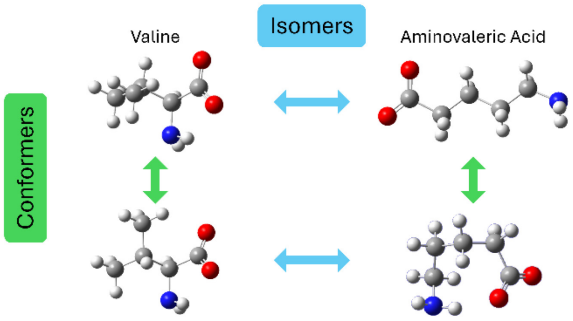

Abstract

We present infrared photodissociation spectra of messenger-tagged, deprotonated valine and deprotonated aminovaleric acid, showing the difference in the vibrational spectra of isomers with the same functional groups. Through comparison of experimental results and density functional theory calculations, we find that the deprotonated states of both valine and aminovaleric acid adopt a configuration in which the carboxylate group forms a hydrogen bond with the amine group. Despite the similarities of the intramolecular hydrogen bonding, the spectra of the two molecules under study are sufficiently different to use the IR signatures of the carboxylate and amine functional groups as a means to distinguish between them. The conformational search in the case of aminovaleric acid is particularly challenging due to the large number of possible conformations induced by torsion around individual carbon-carbon bonds. For both valine and aminovaleric acid, their IR spectra in their deprotonated states suggests that two of the lowest energy conformers are likely to be populated.

Introduction

Infrared (IR) spectroscopy is a powerful tool to investigate molecular structure.[1-4] Examples range from the analysis of naturally occurring functional groups in peptides and proteins, such as amides and their associated vibrational bands,[5-8] to the application of artificial site-specific probes, e.g., nitriles.[9-13] For analytical applications, the detection of signatures of specific functional groups can aid in the identification of molecules in complex mixtures, but significant challenges can remain, even in the case of relatively small molecules.

One analytical application that has recently been proposed[14, 15] is to use a combination of IR spectroscopy and mass spectrometry for unambiguous detection of biosignatures on planetary probes, where an IR spectroscopy channel combined with mass selection could aid in distinguishing molecular ions with the same mass-to-charge ratio and even the same atomic composition, but different molecular structure. An important question in this context is whether molecules with the same functional groups will display vibrational signatures that are sufficiently different to allow distinguishing them. A useful case study to address this question is a comparison of the over 30 different isomers[16] of valine. Four of these have both a carboxylic acid and an amine functional group, namely valine, norvaline, isovaline, and aminovaleric acid (see Supporting Information), and the three former have been detected in both the Murchison meteorite and in Urey-Miller type spark experiments.[17]

As α-amino acids, valine, norvaline, and isovaline are structurally very similar, with the amine group (-NH_2) and the carboxylic acid group (-COOH) connected to the same carbon atom. In typical mass spectrometry applications, such molecules would either occur protonated at the amine group or deprotonated at the carboxylic acid group, and the close vicinity of these two groups results in significant hydrogen bonding (H-bonding) interactions between them.[14, 17] In contrast,

aminovaleric acid (AVA) has the amine and carboxylic acid groups at opposite ends of an aliphatic chain, allowing H-bonding interaction only if this chain bends to form a ring-like structure.

In the present work, we use cryogenic ion vibrational spectroscopy to investigate the H-bonding interaction between carboxylate and amine groups in the deprotonated states of valine and aminovaleric acid. We focus on the antisymmetric OCO stretching, NH_2 bending, and NH stretching modes, and how their behavior differs across these two molecules.

Methods

Here, we provide only a brief description of the experimental setup as it has been described in detail in previous work.[18] We prepared the deprotonated molecular species under study by electrospray ionization (ESI) of 1 mM solutions of L-Val (Sigma-Aldrich) and AVA (Sigma-Aldrich) in 2:1 acetonitrile (Thermo Fisher Scientific) and water, with drops of aqueous potassium hydroxide (Fisher Scientific) added until the solutions reached a pH of 12. All chemicals were used without further purification. Electrosprayed microdroplets entered the vacuum system through a heated desolvation capillary (80 °C), and the ions resulting from desolvation passed through a skimmer. They were then transferred by a series of octopole ion guides and other ion optics into a Paul trap mounted on a closed cycle He cryostat held at ca. 30 K. In the trap, the ions were cooled through collisions with a buffer gas (10% D_2 in He) and tagged with a single N_2 molecule. The ions were ejected from the trap at a repetition rate of 10 Hz.

The trapped ion packet was injected into the acceleration region of a time-of-flight mass spectrometer, and target ions $[Val\text{-}H]^-$ or $[AVA\text{-}H]^-$ (abbreviated M^-) were subsequently mass-selected using an interleaving comb mass gate and irradiated with the output of a tunable OPO/OPA (LaserVision). Photofragments M^- following the reaction

$$M^- \cdot N_2 + \hbar\omega_{IR} \rightarrow M^- + N_2$$

were separated from undissociated parent ions in a two-stage reflectron. Then, the photofragment ion intensity was monitored as a function of IR wavelength on a microchannel plate detector. To improve the signal-to-noise ratio and to ensure reproducibility, multiple spectra taken over several days were averaged for each species. Spectra were calibrated to the known spectrum of acetone[16] using a photoacoustic cell.

Structures of the species under study were calculated using DFT,[19] employing the B3LYP functional[20, 21] and cc-pVTZ basis sets[22, 23] for all atoms. We note that while the reported structures and spectra do not include the tag, exploratory calculations indicate that the tag always binds to the deprotonated carboxylate group and does not significantly change the spectrum (see Supporting Information). The minimum energy structures of deprotonated valine were found using several starting geometries. The conformers of deprotonated aminovaleric acid were found by randomly adjusting the dihedrals of the carbon chain by ten-degree intervals to create 10,000 starting structures, optimizing them at the PM6 semiempirical level, and then narrowing the pool of structures for further optimization based on calculated energies (see Supporting Information). For each minimum energy structure of the deprotonated species, the IR spectrum was calculated based on the harmonic approximation, scaling the frequencies by 0.97, using deprotonated tryptophan as a benchmark.[6] In all calculated spectra, vibrational lines are shown as Lorentzians with 8 cm^{-1} full width at half-maximum. Anharmonic calculations based on the vibrational perturbation theory (VPT2)[24] calculations as implemented in Gaussian 16[25] were used to explore anharmonic couplings between the NH stretching vibrations and the OCO stretching modes. These calculations were done with the B3LYP functional[20, 21] and cc-pVTZ[22, 23] as well as def2TZVPP[26, 27] basis sets to explore basis set effects.

Results and Discussion

Deprotonation of both Val and AVA can be expected to occur preferentially at the carboxylic acid group, based on typical acidities ($pK_a \approx 2$ for carboxylic acids,[28] compared to $pK_a \approx 9$ for amine groups[28]). As a result, a strong intramolecular H-bond forms between the amine group and the carboxylate moiety. The geometries of the lowest lying structures of $[Val\text{-}H]^-$, shown in Figure 1, all possess this structural element. They differ in the orientations of the methyl groups relative to the amine and carboxylate groups, and in the orientations of the amine group relative to the carboxylate group.

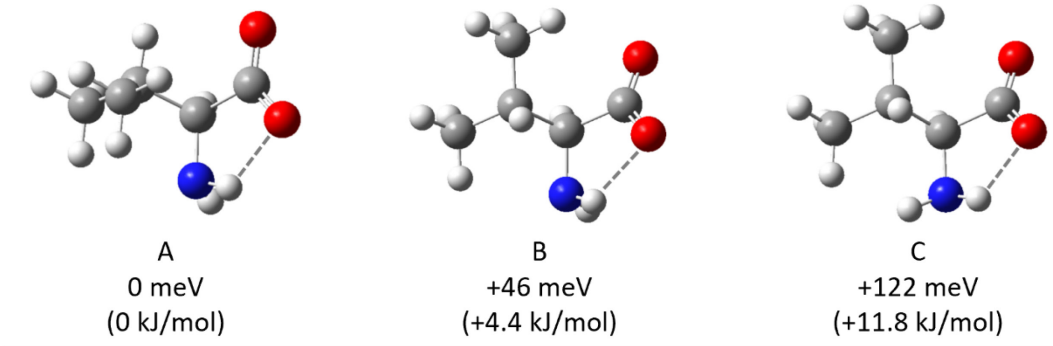

Figure 1. Lowest energy structures of deprotonated L-Val. The zero-point corrected relative energies are given for each structure and the gray dashed lines represent the stabilizing H-bonds. C = gray, H = white, N = blue, O = red.

The experimental spectrum of $[Val\text{-}H]^-\cdot N_2$ (Figure 2) shows two prominent features, at 1632 cm^{-1} (a) and 1581 cm^{-1} (b), a cluster of peaks from 2850-2980 cm^{-1}, and a broad feature centered at 3208 cm^{-1}, which likely contains more than one transition. It is difficult to distinguish between the different conformers based on the IR spectrum alone, since all low-lying structures have very similar IR spectra, and anharmonic calculations with a variety of basis sets show unsatisfactory

agreement with the experiment (see Supporting Information). Nonetheless, the similarity of the calculated IR spectra allows us to assign the observed features. Each structure shows two signatures around 1600 cm^{-1}, which are due to vibrational modes involving both the antisymmetric OCO stretching motion and the NH_2 scissoring motion. The two features represent the two linear combinations of these two local modes, with the higher frequency vibrational mode (a) having a larger amplitude in the OCO group than the lower frequency mode (b) in the case of $[Val\text{-}H]^-$. These features encode the overall structural relationship between the amine group and carboxylate group, and the splitting and intensity distribution between these two features are both characteristic for the structure. The splitting between the features in the experimental spectrum is most consistent with the lowest energy structure, and we tentatively assume that structure A is the dominant conformer. However, feature (a) is unusually broad (ca. 20 cm^{-1}) for a single transition, and it is possible that conformer B may be populated as well, kinetically trapped during cooling in the trap, and could contribute to the spectrum. The barrier between the two conformers is calculated at 194 meV (19 kJ/mol), which is consistent with the notion of kinetic trapping. The relevant transitions in conformers A and B are calculated to differ by 10 cm^{-1}, which is consistent with this hypothesis.

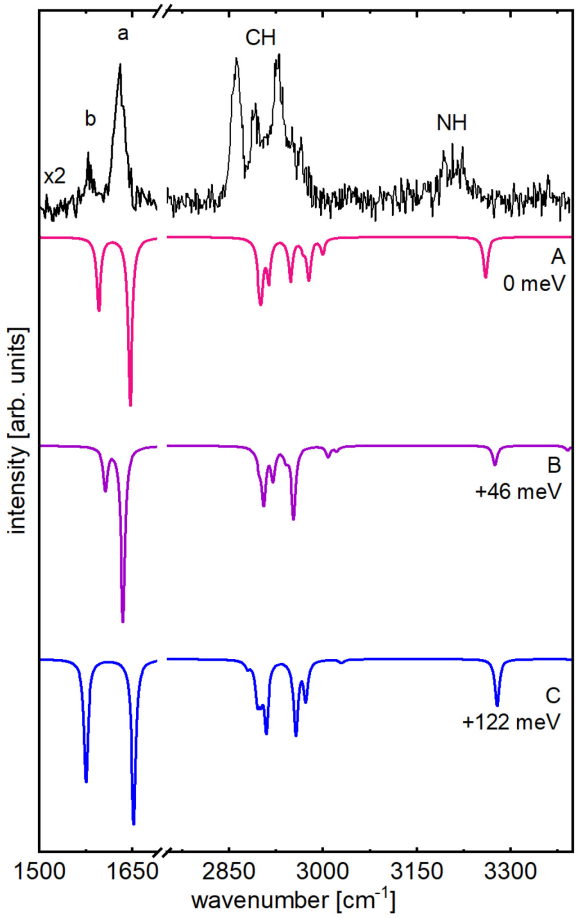

Figure 2. IR photodissociation spectrum of $[Val\text{-}H]^{-}\cdot N_2$ (top, upright) compared to the calculated spectra of different structures of $[Val\text{-}H]^{-}$ (inverted). The structure and relative energy are given for each calculated spectrum with labels as in Figure 1. The low energy region is scaled by a factor of 2 to match the highest intensity peak of the higher energy region.

The region of peaks from 2850-2980 cm^{-1} (labeled CH in Figure 2) contains the CH stretching modes of the methyl groups. The spectral congestion in this region is caused by Fermi interaction of these modes with overtones and combination bands having a total of two quanta in CH bending modes. The lower frequency feature centered at 2862 cm^{-1} contains transitions that are generally deriving their intensity from the symmetric stretching modes of the methyl groups and the CH stretching motion of the CH group closest to the amine. Apart from the latter, which has the lowest

frequency of this group of modes, these modes are generally not strongly localized in specific groups. The peaks at 2890 cm^{-1} and 2927 cm^{-1} and the unresolved shoulders towards higher frequencies belong to similarly delocalized antisymmetric stretching modes of the methyl groups.

The broad feature labeled NH and centered at 3208 cm^{-1} is most likely composed of at least two partially resolved transitions at 3193 cm^{-1} and 3216 cm^{-1}. The symmetric NH stretching transition of the amine group is predicted in this frequency range for all calculated structures. If both conformer A and B were populated in the experiment, they would contribute with symmetric NH stretching transitions that are calculated to be split by 20 cm^{-1}. In this case, the lower frequency, more intense part of the feature would arise from conformer A, while the higher frequency part would originate from conformer B. In principle, broadening of this feature could be caused by effects of the N_2 tag, involving soft modes of the tag itself; however, the most likely binding position of the tag is at the carboxylate group (see Supporting Information), and the atomic displacement amplitudes of the NH stretching vibrational modes are tightly localized to the NH_2 group. It is therefore unlikely that excitation of the NH stretching mode will couple significantly to the soft modes of the N_2 tag. Similarly, different tag positions could lead to shifts in the NH stretching frequency. Typical calculated frequency shifts of the symmetric NH stretching mode upon complexation with N_2 are less than 10 cm^{-1}, and exploratory calculations for various locations of the N_2 tag predict frequency difference below 5 cm^{-1}. An alternative explanation would take into account that this spectral region should contain not only the symmetric NH stretching mode, but also the overtones and combination bands of the NH_2 bending modes, whose fundamental transitions give rise to the signatures observed around 1600 cm^{-1}. Part of the observed broad feature could come from such two-quanta transitions, which would gain intensity through Fermi interactions with the symmetric NH stretching mode. We note that while anharmonic calculations

show that such resonances are indeed predicted in this spectral range, the predicted splitting between the relevant transitions is generally significantly greater than the width of the observed signature, suggesting that the width of this feature is more likely due to the observation of two conformers, most likely A and B. A weak feature around 3360 cm^{-1} can be traced to the antisymmetric NH_2 stretching mode.

In aminovaleric acid (AVA), a linear alkane chain with four CH_2 groups separates its amine and carboxylic acid functional groups, in contrast to Val, where the amine and carboxylic acid moieties are connected to the same carbon atom. Upon deprotonation of the carboxylic acid group, the lowest lying structural conformations are ring structures, connecting the NH_2 and COO^- groups through NH···O H-bonds, while a straight chain structure is significantly higher in energy (Figure 3). The ring structures have very similar relative energies, with the two lowest structures being isoenergetic for all practical purposes.

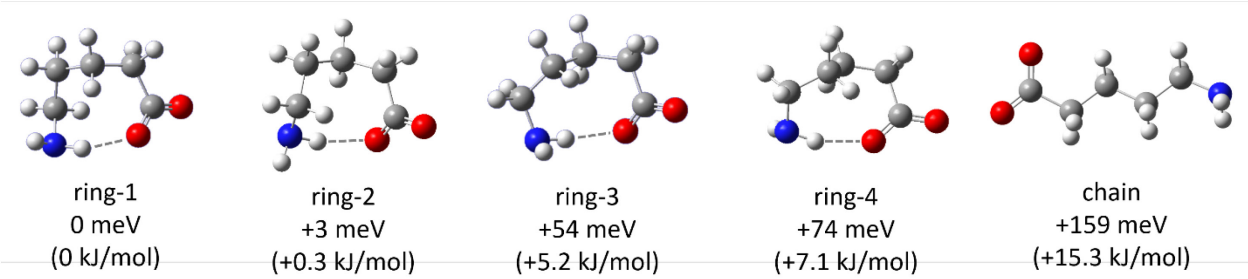

Figure 3. Lowest energy structures of deprotonated AVA, $[AVA-H]^-$. The zero-point corrected relative energies are given for each structure and H-bonds are represented by dashed gray lines. C = gray, H = white, N = blue, O = red.

The IR spectrum of $[AVA-H]^-$ is governed by a prominent peak at 1613 cm^{-1} (Figure 4). This region of the spectrum is sensitive to the interaction between the NH_2 and COO^- groups. In contrast to $[Val-H]^-$, where this interaction is forced by the proximity of these groups, the different

structures of $[AVA-H]^-$ offer some computational access to the effects of their interaction, as ring and chain structures can be readily compared (Figure 4). Similar to $[Val-H]^-$, the calculated peak pattern in this region shows two peaks, which are due to NH_2 scissoring and antisymmetric OCO stretching motions, and the two normal modes of the molecule are due to the two different linear combinations of the local modes. In the experimental spectrum, the lower-intensity, higher frequency component appears as an unresolved shoulder of the more intense feature at 1613 cm^{-1}. The relative intensities of the two modes are different in the ring conformers of $[AVA-H]^-$ compared to $[Val-H]^-$, with the lower frequency feature being the more intense, and the amplitudes of NH_2 scissoring and OCO stretching motions in $[AVA-H]^-$ are nearly identical. In the chain structure of $[AVA-H]^-$, the two vibrational modes appear entirely uncoupled, the amplitudes of both patterns of motion are localized in their respective functional groups, and the more intense mode clearly being the antisymmetric OCO stretching mode. The change in patterns and frequencies upon ring formation shows that the NH_2 scissoring motion is shifted to higher frequencies through interaction with the COO^- group, while the OCO stretching motion experiences a red shift.

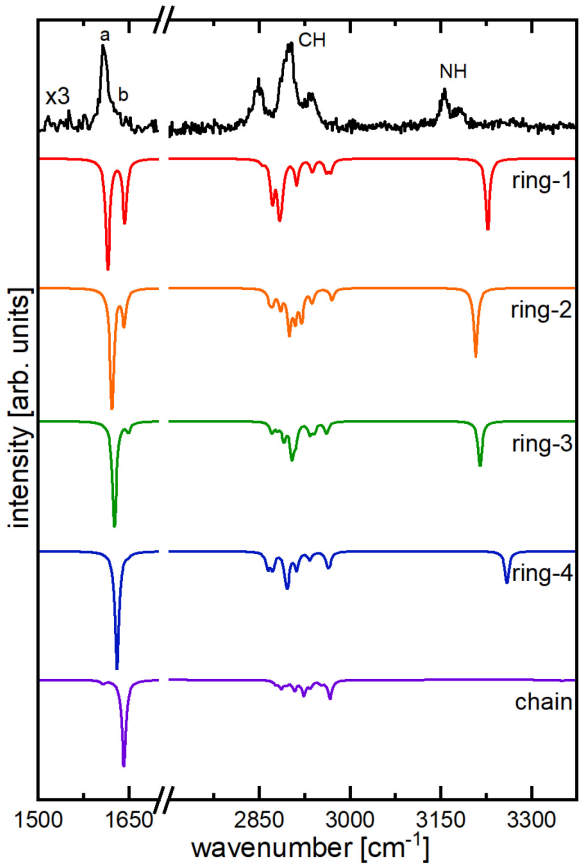

Figure 4. IR photodissociation spectrum of $[AVA\text{-}H]^{-}\cdot N_2$ (top, upright) compared to the calculated spectra of different structures of $[AVA\text{-}H]^{-}$ (inverted, shown with the same vertical scale). The structure is given for each calculated spectrum with labels as in Figure 5. The low energy region is scaled by a factor of 3 to match the highest intensity peak of the higher energy region.

The higher energy region from 2750-3300 cm^{-1} provides some insight into the thermally populated conformers. The cluster of peaks labeled CH in Figure 4 from 2840-2930 cm^{-1} corresponds to the CH stretching modes of the CH_2 groups on the backbone of AVA. Similar to $[Val\text{-}H]^{-}$, this region is not well captured by the scaled harmonic calculations, due to similar anharmonic effects. The lower frequency part of this congested region is mostly composed of linear combinations of the local symmetric CH_2 stretching motions, while the normal modes in the

higher frequency part are largely represented by linear combinations of the local antisymmetric CH_2 stretching modes.

The two peaks labeled NH at 3152 and 3172 cm^{-1} indicate two potential conformers as each calculation predicts one symmetric stretching mode, similar to the case of deprotonated Val. Anharmonic calculations do not recover the experimental spectrum well, and the overtones and combination bands of the OCO stretching/NH_2 bending features are predicted to be higher in frequency than the observed NH stretching signature. For deprotonated AVA, we assign the two peaks to two conformers most likely ring-1 and ring-2, where the relative intensities indicate that ring-2 is the dominant motif. The analogous antisymmetric stretching modes appear to be too weak to be detected in our experiment.

Table 1. Experimental (Calculated in Parentheses) Frequencies in cm^{-1} for $[Val-H]^-$ and $[AVA-H]^-$.

Label[a]	Val	AVA
a	1632 (1646)	1610 (1615-1622)[b]
b	1581 (1595)	1636 (1642-1643)[b]
NH	3208 (3260)[c]	3156, 3180 (3208-3227) [b, d]
CH	2861-2965 (2900-2999)[b]	2842-2932 (2872-2967)[b]

[a] See Figure 2 and Figure 4.

[b] Range of frequencies contributing to this feature.

[c] Peak centroid.

[d] Two features are observed.

In principle, the two normal modes that involve both the NH_2 bending and the antisymmetric OCO stretching local modes are interesting spectroscopic probes of the H-bonding interaction

between the NH_2 and COO^- groups. Both their splitting and their relative intensities are sensitive to this interaction, and these modes will couple to soft, skeletal vibrational modes that modify the distance between those groups and hence their interaction.

Reduced-dimensional VPT2 calculations, where only the NH_2 bending/antisymmetric OCO stretching modes and the NH_2 stretching modes are treated anharmonically, do not describe the spectrum well (see Supporting Information). They generally overestimate the splitting of the two NH_2/OCO modes and yield incorrect intensities for these modes, as well as for their overtones and combination bands. They also show a strong basis set dependence, which is not observed in the scaled harmonic calculations. Exploratory calculations using all vibrational modes in the VPT2 treatment have similar challenges, suggesting that a more sophisticated VPT2-based treatment[4] may be necessary to better recover the spectrum.

The experimental spectra of deprotonated Val and AVA show clear differences for the most intense features in the spectrum. Table 1 lists the relevant signatures, and a visual comparison is shown in Supporting Information. Peak a is the dominant feature of the fingerprint region in each case and has a noticeable shift of 20 cm^{-1} from $[Val\text{-}H]^-$ to $[AVA\text{-}H]^-$, making this feature a promising indicator of which isomer is present. In the higher energy region, the NH signatures are significantly red shifted (by ca. 50 cm^{-1}) from $[Val\text{-}H]^-$ to $[AVA\text{-}H]^-$. Finally, the CH stretching region has a clear pattern difference. As an additional channel of information to add to mass spectrometry platforms, IR spectroscopy can provide a valuable addition to differentiate isomers of valine, even in the case of valine, isovaline, and norvaline, whose calculated spectra (see Supporting Information) are similar in pattern but distinguishable in peak location.

Conclusions

We present the IR spectra of deprotonated valine and one of its chemical analogs, aminovaleric acid. An extensive conformer search shows that aminovaleric acid adopts a ring structure, which allows H-bonding interaction between the amine group and the carboxylate group. By comparing experimental CIVS data with calculated spectra of potential conformers of each isomer, we find that the two lowest energy conformers are likely to contribute to the spectra of both ions. Clear differences in the prominent signatures of the NH_2 bending/OCO stretching modes, the patterns of the CH stretching modes, and the NH stretching features make each isomer clearly distinguishable. Future experimental work building a more complete database encompassing also data on isovaline and norvaline will be necessary for analytical applications on complex samples, as overlapping bands from different isomers will make quantitative analysis more difficult.

The modes involving the NH_2 bending and OCO stretching motions are sensitive probes of the H-bonding interaction between these two functional groups. Surprisingly, and maybe fortuitously, the harmonic calculations in the present work yield better representations of the experimental spectra than one may expect, while our exploratory anharmonic calculations showed that the treatment of these modes is very challenging. The dependence of the spectrum on the relative orientation of these groups, and their anharmonic coupling to soft vibrational modes of the molecule would be interesting targets for future computational work.

ASSOCIATED CONTENT

Supporting Information. The following files are available free of charge: calculated IR spectra of deprotonated valine and selected isomers; calculated structure and IR spectra of N_2-tagged $[Val\text{-}H]^-$; detailed description of the deprotonated aminovaleric acid conformer search including the twelve lowest energy conformers of $[AVA\text{-}H]^-$; calculations treating the NH stretching vibrations and OCO stretching vibrations anharmonically in $[Val\text{-}H]^-$ and $[AVA\text{-}H]^-$; visual comparison of the IR spectra of $[Val\text{-}H]^-$ and $[AVA\text{-}H]^-$; atomic coordinates for lowest energy conformers of $[Val\text{-}H]^-$ and $[AVA\text{-}H]^-$.

AUTHOR INFORMATION

Corresponding Author

*J. Mathias Weber – JILA and Department of Chemistry, University of Colorado, Boulder, Colorado 80309-0440, United States; orcid.org/0000-0002-5493-5886; Phone: +1-303-492-7841; Email: weberjm@jila.colorado.edu

Notes

The authors declare no competing financial interest.

ACKNOWLEDGMENT

Portions of this work were funded by the Jet Propulsion Laboratory, California Institute of Technology, under a contract with the National Aeronautics and Space Administration (80NM0018D0004) and JPL's Strategic University Research Partnership (SURP) program. We gratefully acknowledge partial support from the National Science Foundation under award no. CHE-2154271. L.M.T acknowledges support from a University of Colorado Chemistry

Department Fellowship through the Joseph Addison Sewall Scholarship. This work utilized resources from the University of Colorado Boulder Research Computing Group, which is supported by the National Science Foundation (awards ACI-1532235 and ACI-1532236), the University of Colorado Boulder, and Colorado State University.

REFERENCES

(1) Bocanegra, E. L.; Rana, A.; McCoy, A. B.; Johnson, M. A. Isomer-Specific, Cryogenic Ion Vibrational Spectroscopy Investigation of D- and N-Tagged, Protonated Formic Acid Complexes Using Two-Color, Ir-Ir Photobleaching. *J. Phys. Chem. Lett.* **2024**, *15*, 10944-10949.

(2) LeMessurier, N.; Salzmann, H.; Leversee, R.; Weber, J. M.; Eaves, J. D. Water-Hydrocarbon Interactions in Anionic Pyrene Monohydrate. *J. Phys. Chem. B.* **2024**, *128*, 3200-3210.

(3) Mohamed, A.; Edington, S. C.; Secor, M.; Breton, J. R.; Hammes-Schiffer, S.; Johnson, M. A. Spectroscopic Characterization of the Divalent Metal Docking Motif to Isolated Cyanobenzoate: Direct Observation of Tridentate Binding to Ortho-Cyanobenzoate and Implications for the Cn Response. *J. Phys. Chem. A.* **2023**, *127*, 1413-1421.

(4) Terry, L. M.; Foreman, M. M.; Rasmussen, A. P.; McCoy, A. B.; Weber, J. M. Probing Ion-Receptor Interactions in Halide Complexes of Octamethyl Calix[4]Pyrrole. *J. Am. Chem. Soc.* **2024**, *146*, 12401-12409.

(5) Correia, C. F.; Balaj, P. O.; Scuderi, D.; Maitre, P.; Ohanessian, G. Vibrational Signatures of Protonated, Phosphorylated Amino Acids in the Gas Phase. *J. Am. Chem. Soc.* **2008**, *130*, 3359-3370.

(6) Oomens, J.; Steill, J. D.; Redlich, B. Gas-Phase Ir Spectroscopy of Deprotonated Amino Acids. *J. Am. Chem. Soc.* **2009**, *131*, 4310-4319.

(7) Polfer, N. C.; Paizs, B.; Snoek, L. C.; Compagnon, I.; Suhai, S.; Meijer, G.; von Helden, G.; Oomens, J. Infrared Fingerprint Spectroscopy and Theoretical Studies of Potassium Ion Tagged Amino Acids and Peptides in the Gas Phase. *J. Am. Chem. Soc.* **2005**, *127*, 8571-8579.

(8) Wu, R. H.; McMahon, T. B. An Investigation of Protonation Sites and Conformations of Protonated Amino Acids by Irmpd Spectroscopy. *ChemPhysChem* **2008**, *9*, 2826-2835.

(9) Fafarman, A. T.; Webb, L. J.; Chuang, J. I.; Boxer, S. G. Site-Specific Conversion of Cysteine Thiols into Thiocyanate Creates an Ir Probe for Electric Fields in Proteins. *J. Am. Chem. Soc.* **2006**, *128*, 13356-13357.

(10) Kocheril, P. A.; Wang, H. M.; Lee, D. K.; Naji, N.; Wei, L. Nitrile Vibrational Lifetimes as Probes of Local Electric Fields. *J. Phys. Chem. Lett.* **2024**, *15*, 5306-5314.

(11) Lindquist, B. A.; Furse, K. E.; Corcelli, S. A. Nitrile Groups as Vibrational Probes of Biomolecular Structure and Dynamics: An Overview. *Phys. Chem. Chem. Phys* **2009**, *11*, 8119-8132.

(12) Waegele, M. M.; Culik, R. M.; Gai, F. Site-Specific Spectroscopic Reporters of the Local Electric Field, Hydration, Structure, and Dynamics of Biomolecules. *J. Phys. Chem. Lett.* **2011**, *2*, 2598-2609.

(13) Xu, W. P.; Yi, S. J.; Liu, J.; Jiang, Y. Y.; Huang, J. G. Nitrile-Aminothiol Bioorthogonal near-Infrared Fluorogenic Probes for Ultrasensitive in Vivo Imaging. *Nat. Commun.* **2025**, *16*, 8.

(14) Terry, L. M.; Klumb, M. K.; Nemchick, D. J.; Hodyss, R.; Maiwald, F.; Weber, J. M. Cryogenic Ion Vibrational Spectroscopy of Protonated Valine: Messenger Tag Effects. *J. Phys. Chem. A.* **2024**, *128*, 7137-7144.

(15) Nguyen, T. M.; Ober, D. C.; Balaji, A.; Maiwald, F. W.; Hodyss, R. P.; Madzunkov, S. M.; Okumura, M.; Nemchick, D. J. Infrared Photodissociation Spectroscopy of Water-Tagged Ions with a Widely Tunable Quantum Cascade Laser for Planetary Science Applications. *Anal. Chem.* **2024**, *96*, 8875-8879.

(16) Chu, P. M.; Guenther, F. R.; Rhoderick, G. C.; Lafferty, W. J. Quantitative Infrared Database. In *NIST Chemistry WebBook, NIST Standard Reference Database Number 69*; Mallard, P. J. L. a. W. G., Ed.; National Institute of Standards and Technology.

(17) Wolman, Y.; Haverlan.Wj; Miller, S. L. Non-Protein Amino-Acids from Spark Discharges and Their Comparison with Murchison Meteorite Amino-Acids. *Proc. Natl. Acad. Sci. U.S.A.* **1972**, *69*, 809-811.

(18) Xu, S.; Gozem, S.; Krylov, A. I.; Christopher, C. R.; Weber, J. M. Ligand Influence on the Electronic Spectra of Monocationic Copper-Bipyridine Complexes. *Phys. Chem. Chem. Phys.* **2015**, *17*, 31938-31946.

(19) Parr, R. G.; Yang, W. *Density-Functional Theory of Atoms and Molecules*; Oxford University Press, 1989.

(20) Becke, A. D. Density-Functional Exchange-Energy Approximation with Correct Asymptotic-Behavior. *Phys. Rev. A* **1988**, *38*, 3098-3100.

(21) Lee, C. T.; Yang, W. T.; Parr, R. G. Development of the Colle-Salvetti Correlation-Energy Formula into a Functional of the Electron-Density. *Phys. Rev. B* **1988**, *37*, 785-789.

(22) Dunning, T. H. Gaussian-Basis Sets for Use in Correlated Molecular Calculations .1. The Atoms Boron through Neon and Hydrogen. *J. Chem. Phys.* **1989**, *90*, 1007-1023.

(23) Woon, D. E.; Dunning, T. H. Gaussian-Basis Sets for Use in Correlated Molecular Calculations. III. The Atoms Aluminum through Argon. *J. Chem. Phys.* **1993**, *98*, 1358-1371.

(24) Barone, V. Anharmonic Vibrational Properties by a Fully Automated Second-Order Perturbative Approach. *J. Chem. Phys.* **2005**, *122*, 014108.

(25) Frisch, M. J.; Trucks, G. W.; Schlegel, H. B.; Scuseria, G. E.; Robb, M. A.; Cheeseman, J. R.; Scalmani, G.; Barone, V.; Petersson, G. A.; Nakatsuji, H.; et al. *Gaussian 16 Rev. C.01*; Wallingford, CT, 2016.

(26) Weigend, F.; Ahlrichs, R. Balanced Basis Sets of Split Valence, Triple Zeta Valence and Quadruple Zeta Valence Quality for H to Rn: Design and Assessment of Accuracy. *Physical Chemistry Chemical Physics* **2005**, *7*, 3297-3305.

(27) Weigend, F. Accurate Coulomb-Fitting Basis Sets for H to Rn. *Phys. Chem. Chem. Phys* **2006**, *8*, 1057-1065.

(28) Smith, P. K.; Gorham, A. T.; Smith, E. R. B. Thermodynamic Properties of Solutions of Amino Acids and Related Substances: VII. The Ionization of Some Hydroxyamino Acids and Proline in Aqueous Solution from One to Fifty Degrees. *J. Biol. Chem.* **1942**, *144*, 737-745.